Available online at www.sciencedirect.com

ScienceDirect

journal homepage: www.keaipublishing.com/en/journals/geog;
http://www.jgg09.com/jweb_ddcl_en/EN/volumn/home.shtml

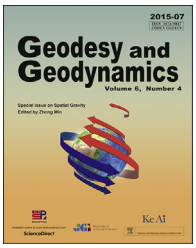

Characteristics of gravity signal and loading effect in China

Yi Shuang*, Sun Wenke

Key Laboratory of Computational Geodynamics, University of Chinese Academy of Sciences, Beijing 100049, China

ARTICLE INFO

Article history:
Received 10 March 2015
Accepted 6 May 2015
Available online 3 July 2015

Keywords:
Gravity change
Loading effect
Gravity Recovery and Climate Experiment (GRACE)
Load love number
Global Positioning System (GPS)
Seasonal variation
Gravity trend in China
Comparison of GRACE and GPS

ABSTRACT

The complex geographical environment in China makes its gravity signals miscellaneous. This work gives a comprehensive representation and explanation in secular trend of gravity change in different regions, the key features of which include positive trend in inner Tibet Plateau and South China and negative trend in North China plain and high mountain Asia (HMA). We also present the patterns of amplitudes and phases of annual and semiannual change. The mechanism underlying the semiannual period is explicitly discussed. The displacement in three directions expressed in terms of geo-potential spherical coefficients and load Love numbers are given. A case study applied with these equations is presented. The results show that Global Positioning System (GPS) observations can be used to compare with Gravity Recovery and Climate Experiment (GRACE) derived displacement and the vertical direction has a signal-noise-ratio of about one order of magnitude larger than the horizontal directions.

1. Introduction

China locates in a complex geographical environment, gradually transiting from the eastern plains to the western highlands, making the topography a distribution of three steps. Tibet Plateau (TP) located in Western China, which is known as the 'world third pole', is still one of the world's most active regions in geology and climate. On the TP, there distribute glaciers, permafrost, lakes and they are all subject to dramatic change: glaciers and permafrost are recently reported retreating rapidly [1], and the lake water level inside the plateau was observed on the rise [2]. In Eastern China, there are seven major river systems, including the world's third and fifth longest river, the Yangtze River and the Yellow River respectively. North China plain (NCP) groundwater loss also can be observed through satellite gravity [3].

The Gravity Recovery and Climate Experiment (GRACE) data have been widely used in the detection of geophysical signals, which mostly come from the cycle of water system, ranging from up to atmosphere and down to ground water.

* *Corresponding author.*
E-mail address: shuangyi.geo@gmail.com (Yi S.).
Peer review under responsibility of Institute of Seismology, China Earthquake Administration.

Production and Hosting by Elsevier on behalf of KeAi

http://dx.doi.org/10.1016/j.geog.2015.05.007

While GRACE has no discrimination on where the signal comes from, it must be careful to separate them, especially for regions with complex geographical environment like China. GRACE can detect geophysical phenomena include change in water reserves, glaciers and possibly the tectonic process in the TP [1]. There has been secular trend map in China, based on GRACE and ground-based gravity measurements [4,5]. But this earlier result did not explicitly discriminate the key features well. In recent years, with the increase in the precision and time range of GRACE data, we get a better understanding of the mass change patterns in China. Scholars have used it to study the changes in glaciers [1,6], in terrestrial water storage [7], in NCP groundwater [3], in inner Tibet Plateau (ITP) [1,2] and in the Yangtze River water reserves [8,9]. Most of the works have been validated by situ or other means of observations.

2. Secular trend in China region

The ground water depletion in North India is so serious that these signals even leak into part of Tibet. Because in this topic we only concentrate on the characteristics in China region, this interference should be excluded. To separate the negative signals from India ground water and high mountain Asia (HMA) glaciers, we use an iterative method to separate the signals belonging to North India. The secular trend of equal water height (EWH) change after the extraction of Indian signals is shown in Fig. 1 and the extracted India water signal is plotted in the inner graph. The (GRACE RL05 model from 2003 to 2013 solved by the University of Texas at Austin, Center for Space Research (UT-CSR) is used. In this study, the decorrelation filter P4M6 [10] and the 300 km Gauss smoothing filter [11] are adopted.

The India water signal is separated by these steps: first, the grids covering the North India is chosen and assigned with a tried negative mass; second, the tried mass is expanded into spherical harmonics and then applied with the same smooth techniques described above, and we can get an smoothed observation from the tried mass; third, the tried mass is adjusted iteratively until we make its signal close to GRACE observation in this area. As a result, we get a real mass in North India, rather than a smoothed one, and the mass is subtracted in the GRACE observations to get our final trend map.

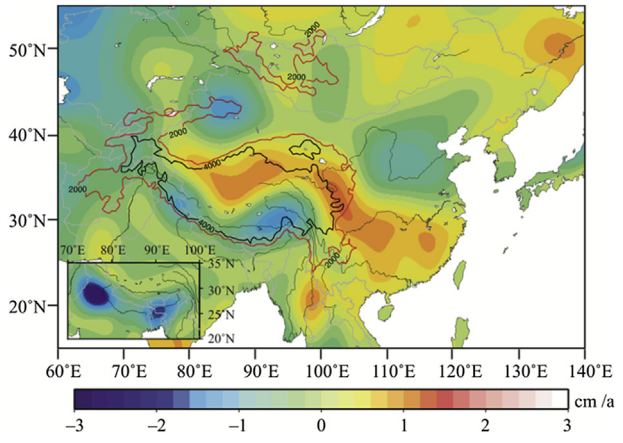

Fig. 1 – Secular trend of EWH in China region. The signals from India water are extracted and plotted in the inner graph. Bold curves are contours of topography (2000 m and 4000 m).

We can find such dominant characteristics: the negative signals from melt of glaciers in Tianshan and periphery of TP (including Pamir, Himalaya and Nyenchen Tanglha Mountain) and from ground water depletion in NCP; The positive signals cover most of inner Tibet and extend out across Sichuan Basin into South China.

The water crisis in NCP is an imbalance between demand and supply. In China there are 20% of the world's population that are dependent on 5–7% of global freshwater resources [12]. Therefore, many regions in China are facing issues of overexploitation of groundwater, which further triggers the issue of ground subsidence [13]. NCP is one of the largest irrigation areas in the world and is subjected to intensive groundwater-based irrigation. Based on the GRACE derived terrestrial water storage and simulated soil moisture estimates, the groundwater depletion rate in North China was 8.3 ± 1.1 km^3/a from 2003 to 2010 [3].

Our latest work showed that the glaciers in HMA are melting at a rate of −35.0 ± 5.8 Gt/a and the Indian underground water is being lost at a rate of −30.6 ± 5.0 Gt/a. Global warming has accelerated the melting rate of glaciers in HMA. In Fig. 1 it is clearly illustrated that the glaciers in Tianshan Mountain and Nyenchen Tanglha Mountain are suffering from the most severe retreating magnitude. Along the Himalaya there are negative signals, implying an overall reduction in glacier capacity. Contrary to this mass loss, in the ITP, we got a larger positive signal (30 Gt/a) and declared the difficulty in explaining it under current knowledge because several factors are still unclear in the ITP. The positive signal may come from water storage increase (including lakes, permafrost and groundwater) and inflow of crust.

The variance of water storage in Yangtze River has been reported strong correlated with El Niño–Southern Oscillation (ENSO), with a phase lag of 7–8 months [9]. But the long trend in South China is less discussed. We declare a positive trend in South China. It is likely a result of increase in precipitation and the Three Gorges Dam has blocked a certain volume of water in the midstream of the Yangtze River since 2003. In fact, possibly linked with global warming, ever since 1901, averaged precipitation has increased over the mid-latitude land areas of the Northern Hemisphere [14].

3. Periods

We stack the observations by month to get the yearly variance. The monthly EWH results are fitted by a function of one long trend with three periods:

$$f(t) = at + b + \sum_i A_i \cos\left(\frac{2\pi}{T_i}(t - \varphi_i)\right) \quad (1)$$

here, $T_1 = 1$ for annual period, $T_2 = 0.5$ for semiannual period and $T_3 = 5$ for 5-year period. A_i and φ_i are their corresponding amplitude and phase.

The results of amplitudes and phases are plotted in Fig. 2. The annual variance of mass concentrates in south of TP,

where the high mountain blocks the humid wind blowing from the India Ocean and brings here one of the most intense precipitation in the world. We can also find some peaks in Pamir and South China.

The semiannual period is also plotted here. The driving force of annual change is the alteration of seasons, one warm and one cold in a year. It is hard to understand which brings the semiannual change. In fact, it is not real but only a result of mathematical decomposition, i.e., if the yearly signal is not a perfect sine or cosine curve, we will inevitably get a semiannual component.

The semiannual component is weaker than the annual component in amplitude so it only put a modification on the shape of annual change. Based on the relations between phases of annual of semiannual change, we divide them into four groups, which are demonstrated in Fig. 3:

1. The peaks of annual and semiannual change are coincident. So the maximum of the seasonal variation is strengthened (a larger peak value but a shorter peak period) and the minimum weakened. This is the change pattern of point-c in Fig. 3. This happens when the precipitation concentrates only in a few months.
2. The minima of annual and semiannual change are coincident. So the maximum of the seasonal variation is weakened (a smaller peak value but a longer peak period) and the minimum strengthened. This is the change pattern of point-*a*. This happens when the precipitation is moderate and lasts for a long time.
3. The peak of annual change is a little ahead of the peak of semiannual change. So the mass accumulates smoothly but loss rapidly. This is the change pattern of point-*d*.
4. The peak of annual change is a little delayed of the peak of semiannual change. So the mass accumulates rapidly but loss smoothly. This is the change pattern of point-*b*.

The annual phase can tell that several climate factors control the water storage in China. India is apparently completely controlled by the India monsoon. From west we can clearly find a boundary, starting along 32° E, then south and west border of Pamir and ending in Tianshan. This marks the dividing line between westerlies-impacting zone and monsoon-impacting zone, across which the peak month changes from April to September very sharply. In TP there is plateau mountain climate, with an earlier peak month in the East Himalaya, implying a unique changing characteristic of mountain glaciers.

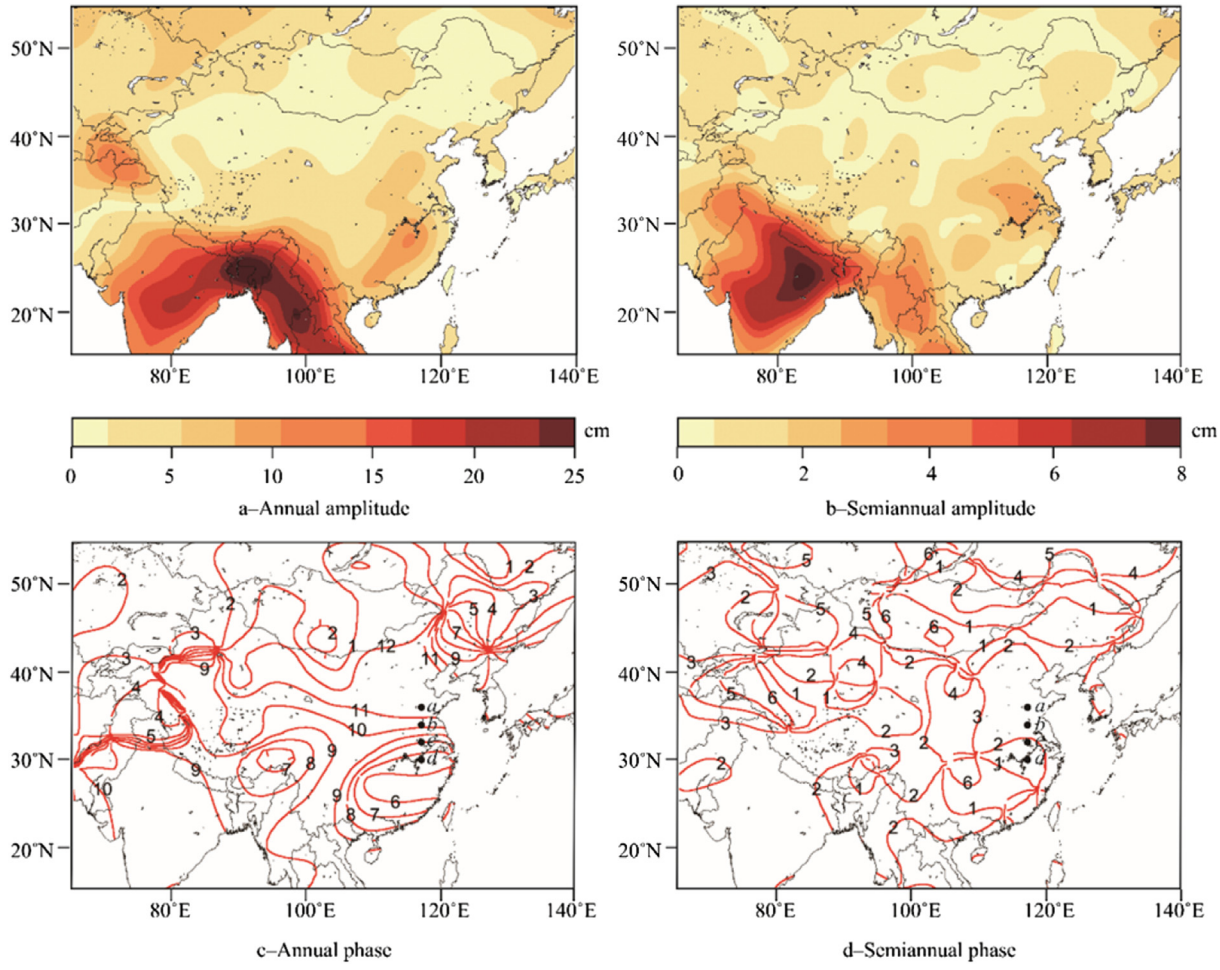

Fig. 2 – Amplitude and phase of annual and semiannual EWH change. In the phase subgraphs, contours are in unit of month. Point *a*–*d* are specified samples with their yearly series plotted in Fig. 3.

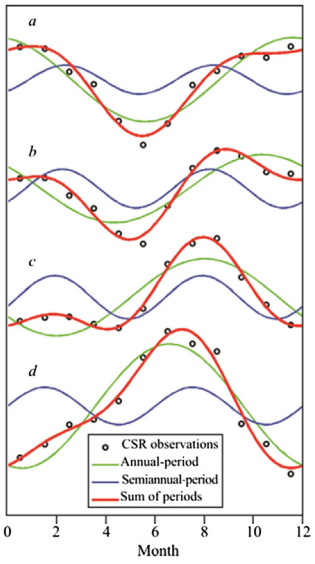

Fig. 3 – Annual change of EWH in specified points, the location of which is annotated in Fig. 2.

The southeast and northwest monsoons together put an impact on the eastern half of China, making the South China humid subtropical monsoon climate with an earliest peak month in May and Northeast China temperate monsoon climate with a gradually delayed peak month from northeast to southwest.

We proposed a 5-year period in the Pamir glacier, likely to be caused by Indian monsoons in a earlier study [1]. This large interannual variance can bias us in determining the secular change, especially when the observations are limited in time. A case study of Pamir glacier is discussed in that study. We extend the research range in Fig. 4 and find this 5-year period also exists in many other places. It is interesting that these places surround China and no significant signals of 5-year period can be found within the scope of China.

4. Surface loadings

The terrestrial water storage puts a seasonal surface load on the Earth. So the ground will have a corresponding time-varying deformation in different seasons, which is detectable by Global Positioning System (GPS). As a result, the comparison of GRACE and GPS has been studied by many groups. Liao [15] compared the GRACE-derived seasonal vertical deformation with 42 GPS stations in China and found a consistency in both amplitude and phase in most stations.

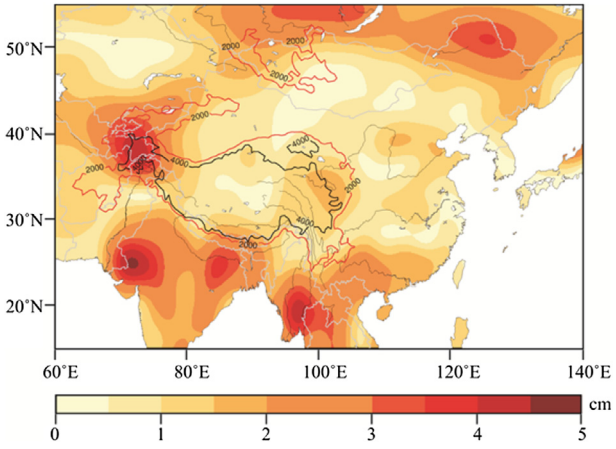

Fig. 4 – Amplitude of 5-year period in China.

GRACE measurements can also be used to remove the hydrological effect in GPS measurements, especially when the GPS observations are limited, mostly once per year, in which case seasonal variations for campaign GPS measurements cannot be well constrained [16]. Fu [16] compared the GPS and GRACE measurements in Nepal Himalaya and found that after subtracting GRACE-derived vertical displacement from the GPS observed time, the average weighted root mean squares (WRMS) is approximate 45% deduced. Sheng [17] studied 13 continuous GPS stations in Western Yunnan Province, China. They adopted GRACE data to extract the land water deformation in GPS observations and found a 67% decrease in the GPS error.

5. Principle

With load Love numbers and geo-potential spherical coefficients, we can calculate the displacement in the directions of height (Δh), east (Δe) and north (Δn) due to the mass load. The equations are derived from Kusche [18].

$$\Delta h(\theta,\phi) = a\sum_{l=1}^{\infty}\sum_{m=0}^{l}\tilde{P}_{lm}(\cos\theta)\left\{C_{lm}^{g}\cos m\phi + S_{lm}^{g}\sin m\phi\right\}\left(\frac{h_l'}{1+k_l'}\right) \tag{2}$$

$$\Delta e(\theta,\phi) = \frac{a}{\sin\theta}\sum_{l=1}^{\infty}\sum_{m=0}^{l}m\tilde{P}_{lm}(\cos\theta)\left\{-C_{lm}^{g}\sin m\phi + S_{lm}^{g}\cos m\phi\right\} \times\left(\frac{l_l'}{1+k_l'}\right) \tag{3}$$

$$\Delta n(\theta,\phi) = -a\sum_{l=1}^{\infty}\sum_{m=0}^{l}\frac{\partial}{\partial\theta}\tilde{P}_{lm}(\cos\theta)\left\{C_{lm}^{g}\cos m\phi + S_{lm}^{g}\sin m\phi\right\} \times\left(\frac{l_l'}{1+k_l'}\right) \tag{4}$$

where $\tilde{P}_{lm}$ is Normalized associated Legendre polynomials (NALP). a is the radius of the Earth. C_{lm}^{g} and S_{lm}^{g} are geo-potential coefficients. k'_l, h'_l and l'_l are load Love numbers. θ and ϕ are colatitude and longitude, respectively. $\frac{\partial}{\partial\theta}\tilde{P}_{lm}(\cos\theta)$ is first partial derivatives (FPD) of NALP.

We can solve NALP by the recurrence formula, which can be found in many literatures and we do not bother to repeat this part. Since the FPD is less familiar, its solution method is given here. It can be solved by following equations, once we get the values of NALP:

$$\frac{\partial}{\partial\theta}\tilde{P}_n^n(x) = n\cot\theta\tilde{P}_n^n(\cos\theta) \tag{5}$$

$$\frac{\partial}{\partial\theta}\tilde{P}_n^m(\cos\theta) = -\frac{1}{\sin\theta}\sqrt{\frac{(n-m)(n+m)(2n+1)}{(2n-1)}}\tilde{P}_{n-1}^m(\cos\theta) + n\cot\theta\tilde{P}_n^m(\cos\theta) \tag{6}$$

Load Love numbers are provided in Farrell [19]. The computation is based on the center of mass of solid earth

frame. To convert it into the center of figure (CF) frame, we adopt a different value in degree 1: $l'_1 = 0.134$, $h'_1 = -0.269$. The CF frame consists with an ideal no-net translation projected along any axis [18].

6. Results

The GPS and leveling can give the displacement in these three directions [20]. So it is easy to compare these results with GRACE based on the equations we have got. A demonstration case is presented here to show the results of the equations above. The mass variance in June and its loading effect are shown in Fig. 5.

In Fig. 5, the EWH with a value of 20 cm can cause a height displacement in a value of 8 mm. Their patterns are quite similar, but in the opposite sign. This is because a mass excess will result in a ground subsidence and vice versa. The horizontal movement has quite a different pattern. But it is still not hard to understand. Taken displacement in North India as an example, in June there is a mass deficit in this place. The compressed ground (in heavier load seasons) will expand when the load is off, not only result in an uplift in the height, but also a horizontal extension. That means the northern part will go further north (positive) and eastern part will go further east (positive). This explains why we get a positive sign in the north and east, but a negative sign in the south and west.

The horizontal movement is much smaller than vertical movement. Taken the equipment precision into consideration, the seasonal variation in horizontal direction is relatively harder to discern, compared with the distinct seasonal variance in vertical direction. There has been about 2000 GPS stations giving horizontal crustal deformation in China mainland [21] and these data can give an overall and detailed comparison with GRACE. However the secular trend need observations in a longer time range. In fact, the secular trend of movement may be mostly caused by tectonic process,

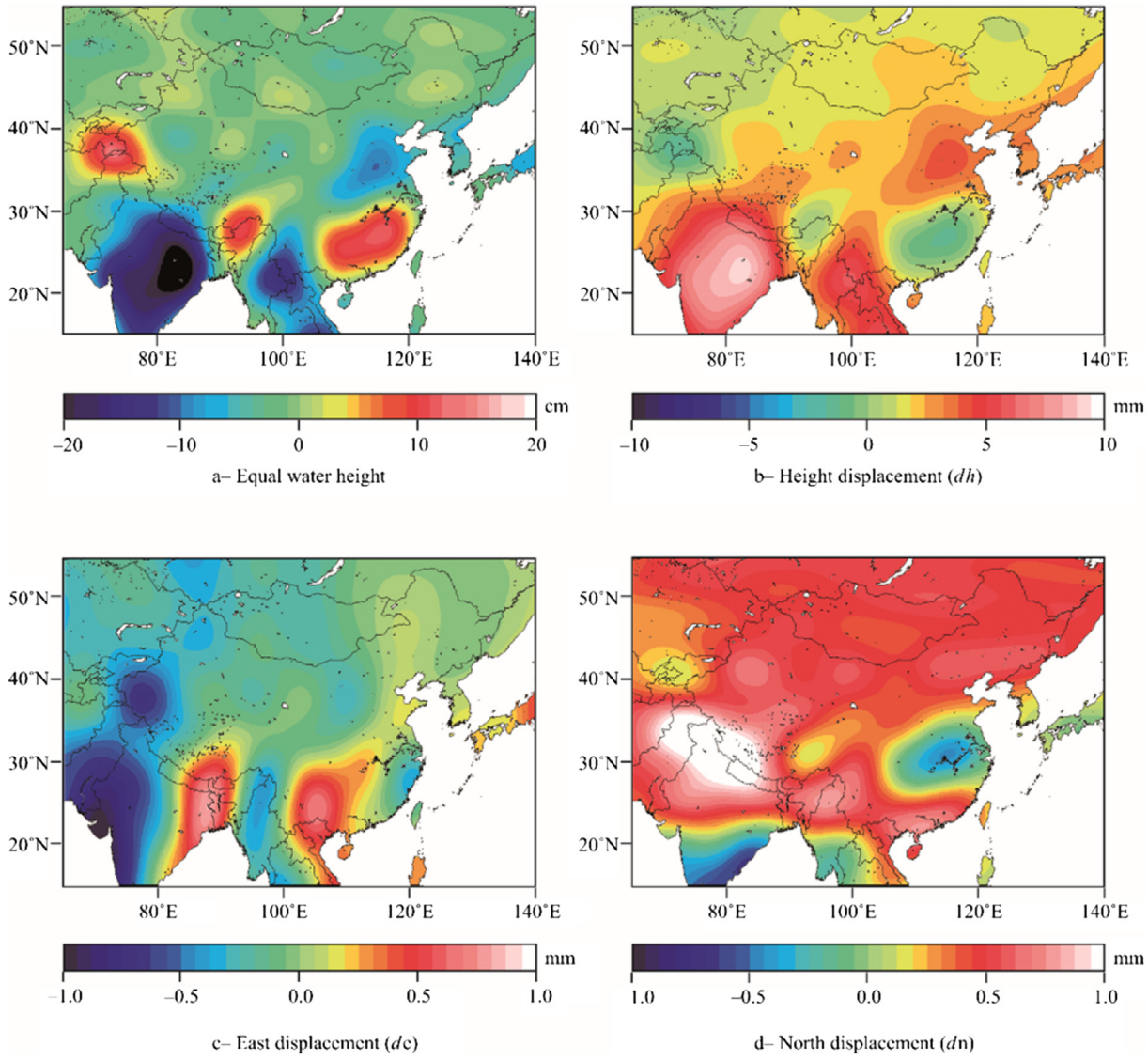

Fig. 5 – Equal water height (in cm) in June and its loading effect (in mm). Note the difference in the unit and range of color scale.

rather than accumulated loading effect. This condition is very likely in southwest China. As a result, the trends of GRACE and GPS measurements reflect different mechanisms.

7. Conclusions

In this paper, we discuss the general mass trend pattern in China region. There are two positive (in ITP and South China) and two negative signals (in HMA and NCP). Also we give the amplitude and phase patterns of annual and semiannual periods and amplitude of 5-year period. The amplitude patterns of mass have a strong relationship with the distribution of precipitation. The explanation of semiannual period is given and the underlying phenomena between the phase of annual and semiannual signals are presented.

In the end, we have derived the equations involving load Love numbers to calculate the displacement in three directions caused by surface load. A case is given. We discuss the mechanism of how the patterns form. We conclude that load can cause seasonal vertical displacement nearly 10 mm and is easy to discern, but the seasonal horizontal displacement is harder to discriminate, with a value of about 1 mm, almost at the same level as secular trend.

Acknowledgment

This research was supported financially by the National Natural Science Foundation of China (41174063, 41331066 and 41474059), the CAS/CAFEA International Partnership Program for Creative Research Teams (KZZD-EW-TZ-19), and the SKLGED Foundation (2014-1-1-E).

REFERENCES

[1] Yi Shuang, Sun Wenke. Evaluation of glacier changes in high-mountain Asia based on 10 year GRACE RL05 models. J Geophys Res Solid Earth 2014;119(3):2504–17.
[2] Zhang Guoqing, Yao Tandong, Xie Hongjie, Kang Shichang, Lei Yanbin. Increased mass over the Tibetan Plateau: from lakes or glaciers? Geophys Res Lett 2013;40(10):2125–30.
[3] Feng Wei, Zhong Min, Lemoine Jean-Michel, Biancale Richard, Hsu Hou-Tse, Xia Jun. Evaluation of groundwater depletion in North China using the Gravity Recovery and Climate Experiment (GRACE) data and ground-based measurements. Water Resour Res 2013;49(4):2110–8.
[4] Xing Lelin, Li Hui, Xuan Songbai, Kang Kaixuan, Liu Xiaoling. Long-term gravity changes in Chinese mainland from GRACE and ground-based gravity measurements. Geodesy Geodyn 2011;2(3):61–70.
[5] Zhong Min, Duan Jianbin, Xu Houze, Peng Peng, Yan Haoming, Zhu Yaozhong. Trend of China land water storage redistribution at medi- and large-spatial scales in recent five years by satellite gravity observations. Chin Sci Bull 2009;54(5):816–21.
[6] Matsuo Koji, Heki Kosuke. Time-variable ice loss in Asian high mountains from satellite gravimetry. Earth Planet Sci Lett 2010;290(1):30–6.
[7] Llovel W, Becker M, Cazenave A, Crétaux Jean-François, Ramillien G. Global land water storage change from GRACE over 2002–2009; inference on sea level. Comptes Rendus Geosci 2010;342(3):179–88.
[8] Hu Xiaogong, Chen Jianli, Zhou Yonghong, Huang Cheng, Liao Xinhao. Seasonal water storage change of the Yangtze River basin detected by GRACE. Sci China Ser D 2006;49(5):483–91.
[9] Zhang Zizhan, Chao BF, Chen Jianli, Wilson CR. Terrestrial water storage Anomalies of Yangtze River Basin droughts observed by GRACE and connections with ENSO. Glob Planet Change 2015;126:3545.
[10] Swenson S, Wahr J. Post-processing removal of correlated errors in GRACE data. Geophys Res Lett 2006;33(8).
[11] Wahr J, Molenaar M, Bryan F. Time variability of the Earth's gravity field: hydrological and oceanic effects and their possible detection using GRACE. J Geophys Research-Solid Earth 1998;103(B12):30205–29.
[12] Qiu J. China faces up to groundwater crisis. Nature 2010;466(7304). 308–308.
[13] Hu RL, Yue ZQ, Wang LC, Wang SJ. Review on current status and challenging issues of land subsidence in China. Eng Geol 2004;76(1–2):65–77.
[14] Hartmann DL, Klein Tank AMG, Rusticucci M, Alexander LV, Brönnimann S, Charabi Y, et al. Observations: atmosphere and surface. Cambridge, United Kingdom and New York, NY, USA: Cambridge University Press; 2013. p. 159–254.
[15] Liao Haihua, Zhong Min, Zhou Xuhua. Climate-driven annual vertical deformation of the solid Earth calculated from GRACE. Chin J Geophys 2010;53(5):1091–8 [in Chinese].
[16] Fu Y, Freymueller JT. Seasonal and long-term vertical deformation in the Nepal Himalaya constrained by GPS and GRACE measurements. J Geophys Res 2012;117:B03407. http://dx.doi.org/10.1029/2011JB008925.
[17] Sheng Chuanzhen, Gan Weijun, Liang Shiming, Chen Weitao, Xiao Genru. Identification and elimination of non-tectonic curstal deformation caused by land water from GPS time series in the western Yunnan province based on GRACE observations. Chin J Geophys 2014;57(1):42–52 [in Chinese].
[18] Kusche J, Schrama E. Surface mass redistribution inversion from global GPS deformation and Gravity Recovery and Climate Experiment (GRACE) gravity data. J Geophys Res Solid Earth 2005;110(B9). 1978–2012.
[19] Farrell WE. Deformation of the Earth by surface loads. Rev Geophys 1972;10(3):761–97.
[20] Wang Qingliang, Ji Lingyun, Wang Shuangxu. Present-day 3D deformation field of Northeast China, observed by GPS and leveling. Geodesy Geodyn 2014;5(3):34–40.
[21] Wang Wei, Wang Dijin, Zhao Bin, Huang Yong, Zhang Caihong, Tan Kai, et al. Horizontal crustal deformation in Chinese Mainland analyzed by CMONOC GPS data from 2009-2013. Geodesy Geodyn 2014;5(3):41–5.

YI Shuang, a PhD candidate at University of Chinese Academy of Sciences. He graduated from the School of Geodesy and Geometrics, Wuhan University in 2011 and got the bachelor degree of science in solid geophysics. Since 2011, he has been enrolled in the College of Earth Science, University of Chinese Academy of Sciences for M.S-Ph.D. His research areas include: the characteristics of mass change and modern geodynamics in the Tibetan Plateau; global climate change and the response of sea level, land ice and land water; the process and analysis of GRACE gravity data. He has published two papers in Journal of Geophysical Research and Geophysical Research Letters respectively.